Supplemental methods and results

Human lung conventional dendritic cells orchestrate lymphoid neogenesis during COPD

Authors: Thomas Naessens, Yannick Morias[*], Eva Hamrud[*], Ulf Gehrmann, Ramachandramouli Budida, Johan Mattsson, Tina Baker, Gabriel Skogberg, Elisabeth Israelsson, Kristofer Thörn, Martijn J. Schuijs, Bastian Angermann, Faye Melville, Karl J Staples, Danen M Cunoosamy[#] and Bart N Lambrecht[#]

*Authors contributed equally to this paper

#Authors co-supervised the study

Supplemental Methods

Human lung samples

Lung samples were obtained from 35 non-obstructed control subjects (i.e. normal lung function, among whom 8 never-smokers, 1 current smoker and 26 former smokers) and 12 patients with COPD undergoing lung surgery, either for resection of a solitary tumor (24 control subjects and 7 COPD GOLD II subjects) or transplantation for very severe COPD (5 COPD GOLD IV subjects) at the Sahlgrenska University Hospital, Gothenburg, Sweden. All subjects underwent preoperative post-bronchodilator spirometry. Subjects were categorized by based on the 2001 classification of the Global Initiative for Chronic Obstructive Lung Disease (GOLD) (1). In case of resected tissue, macroscopically healthy lung was sampled. We defined ex-smokers as having quit smoking habits for at least 6 months before surgery.

Human lung sample processing

Lung tissue was extensively flushed with PBS (Invitrogen) to remove excessive blood contamination and alveolar cells. The flushed tissue was subsequently cut into small pieces (0,5 cm x 0,5 cm) and incubated in a digestion buffer, containing 1mg/ml Collagenase D (Sigma-Aldrich) in RPMI medium (Invitrogen), for 30 minutes at 37°C. Afterwards, the lung tissue pieces were minced over a 100 µm cell strainer (Miltenyi Biotec) to obtain a single cell suspension.

Single-cell RNA sequencing of human lung myeloid cells

FACS-sorted myeloid subpopulations were stained with Hoechst 33342 and Propidium Iodide dye mix (Invitrogen, MA, USA) and diluted to 20,000 cells/mL. The cells were dispensed into nanowells using the ICELL8 Single-Cell System (Takara Bio, Japan), and

single live cells were identified using CellSelect software (WaferGen, CA, USA). After a freeze-thaw cycle, the cells were processed for RT-PCR and cDNA amplification according to the manufacturer's instructions. The cDNA amplicons were then pooled and concentrated using Zymo DNA Clean & Concentrator^{TM}-5 kit (Zymo Research, CA, USA) followed by cDNA purification using 0.6X AMPure XP beads (Beckman Coulter, IN, USA) and quantification using Qubit dsDNA HS Assay Kit on the Qubit fluorometer (Thermo Fisher, MA, USA). The cDNA was quality checked using HS NGS kit on a Fragment Analyzer (Agilent, CA, USA). The purified cDNA was subsequently used for Nextera XT (Illumina, CA, USA) library preparation and amplification. A total of three lung tissues were processed individually for the library preparation. The quality and quantity of the libraries was analyzed using HS NGS Fragment Analyzer and Qubit dsDNA HS Assay Kit respectively. Sample libraries were pooled in equimolar concentrations and diluted and denatured according to Illumina guidelines. Sequencing was performed using a High Output 150 cycle kit on an Illumina NextSeq550 using 26 cycles for read1, and 126 cycles for read2.

Raw sequence processing and quality control. RNA-seq fastq files were processed using bcbio-nextgen (version 1.1.0) (bcbio-nextgen. Validated, scalable, community developed variant calling, RNA-seq and small RNA analysis. Available from: https://github.com/chapmanb/bcbio-nextgen) where reads were mapped to the human genome build hg38 (GRCh38.92 version 25) using hisat2 (version 2.1.0) (2). For the bulk dataset this yielded between 37.2 – 64.9 M mapped reads per sample (with a mean of 49.4 M). No filtering of samples or genes was performed on the bulk RNA sequencing data. For the single cell dataset, 180 M reads aligned to genes. Gene level quantifications, counts and transcript per million (TPM), were generated with featurecounts (version 1.4.4) (3) and sailfish (version 0.10.1) (4), respectively, all within bcbio. The single cell dataset was additionally demultiplexed using UMIs with the umis (version 1.0.0), also within the bcbio framework.

Quality control included filtering by, the number of genes per cell, mitochondrial gene contribution and minimum gene representation across cells.

Single cell sequencing data clustering and cluster identification. For the single cell data, most analyses were performed using Seurat toolkit (4) (https://satijalab.org/seurat/, version 3.1.0) available in R (R version 3.5.1). Single cell data was processed to regress out unwanted sources of variation. Cells from the three donors were aggregated into separate Seurat objects, these were then aligned to each other using canonical correlation analysis. Clustering was conducted using a graph-based clustering approach within the framework of Seurat. 14 clusters that were found were used for all subsequent analysis and visualized using the Seurat function TSNEplot. All plots were made using R (version 3.5.2, www.r-project.org) and Seurat (version 3.1.0). Unique marker genes per cluster were extracted with the Seurat function FindAllMarkers and the top 20 genes which displayed the highest log fold change in expression between clusters were extracted. A phylogenetic tree relating to the 'average' cell from each identity class was constructed from the dataset using the Seurat function BuildClusterTree and the resulting scaled expression data for the top 20 genes per cluster were plotted using the Seurat function DoHeatmap. To confirm cluster identities, published gene signatures for blood DC subtypes from Villani *et al.* (5) and Zilionis *et al.* (6) were matched against our clusters. The gene lists from Villani *et al.* were first filtered to remove any blood-specific genes that did not appear in any of our single cell dataset. A signature score was then calculated for each signature and cluster using the Seurat function *AddModuleScore*. Resulting scores were plotted using the Seurat function *VlnPlot*.

Next Generation RNA transcriptome Sequencing of human lung DC subsets

Total RNA preparation. Sorted lung DC subsets were resuspended in 350 µl of RLT Plus buffer (Qiagen) and stored at −80° C. Cell lysates were thawed, and total RNA was

extracted using RNeasy Plus Micro Kit (Qiagen) according to the manufacturer's protocol. RNA quality and quantity were assessed on the Fragment Analyzer platform (AATI) using high sensitivity RNA analysis kit. Only samples with RNA Integrity Number >8 were subsequently used.

Whole transcriptome profiling by RNA sequencing. 1.5 ng of total RNA was used as input to create total RNA libraries using Ovation® SoLo RNA-Seq System (NuGEN Technologies) according to the manufacturer's protocol. Libraries were validated on the Fragment Analyzer platform (AATI) using standard sensitivity NGS fragment analysis kit and the concentration was determined using Quant-iT dsDNA High Sensitivity assay kit on the Qubit fluorometer (Thermo Fisher). Sample libraries were pooled in equimolar concentrations, diluted, and denatured according to Illumina guidelines. Sequencing was performed using a High Output Kit v2 (150 cycles) on an Illumina NextSeq500.

Data analysis. The TPM (transcript per million) counts from the bulk RNA sequencing dataset of the FACs-sorted cDC1, cDC2, pDC and $CD14^+$ monocytes were log transformed and expression of genes of interest were plotted as a heatmap using the function *pheatmap* (7) (pheatmap: Pretty Heatmaps, version 0.12, https://CRAN.R-project.org/package=pheatmap). Ingenuity Pathway Analysis (IPA; QIAGEN) was used to functionally categorize differentially expressed genes and to biocomputationally identify putative upstream regulators responsible for differential gene expression signatures.

Flow cytometry

Extracellular surface marker staining. Lung single cell suspensions were incubated with Aqua LIVE/DEAD (Thermofisher) in PBS for 15 minutes at 4°C. After 2 washing steps with PBS, cells were stained in PBS containing 0,5% Fetal Calf Serum (FCS) (Invitrogen) and 2mM EDTA (Invitrogen) with anti-human CD45-BV605 (clone HI30), HLA-

DR-BV786 (clone G46-6), CD3ε-FITC (clone UCHT1), CD19-FITC (clone HIB19), CD56-FITC (clone B159), CD66b-FITC (clone G10F5), CD16-PerCP-Cy5.5 (clone 3G8), CD11c-PE-CF594 (clone B-ly6), CD141-BV711 (clone 1A4), CD3ε-PE-CF594 (clone UCHT1), ICOS-BV421 (clone DX29), CXCR5-PerCP-Cy5.5 (clone RF8B2), CXCR5-BUV395 (clone RF8B2), CXCR4-BUV395 (clone 12G5), PD-L1-BUV395 (clone MIH1), FcεRI-PE (clone AER37) (all from BD Biosciences), CD123-PE-Cy7 (clone 6H6), CD172a-APC (clone 15-414), CD14-AF700 (clone 63D3), CD1c-BV421 (L161), CLEC9a-APC (clone 8F9), XCR1-PE (clone S15046E), CD206-APC (clone 15-2), CD1a-PE-Cy7 (clone HI149), PD-1-BV711 (clone EH12.2H7), OX40-PE-Cy7 (clone Ber-ACT35), EBI2-PE (clone SA313E4), ICOSL-PE-Cy7 (clone 2D3), CD1a-PE-Cy7 (clone HI149) (all from Biolegend) and OX40L-PE (clone ANC10G1) (Ancell) for 30 minutes at 4°C.

Intracellular cytokine staining. To assess the expression of intracellular cytokines, cells were stimulated with PMA (30ng/ml) and ionomycin (1μg/ml) (both from Sigma) for 6h in the presence of GolgiPlug and GolgiStop (both from BD Biosciences) for the last 4h. After stimulation, extracellular surface markers were stained before cells were fixed and permeabilized (Fixation/Permeabilization Buffer Set, BD Biosciences). Next, cells were stained with anti-human IL-21-eFluor660 (clone 3A3-N2) (eBioscience), CXCL13-PE (clone 53610) (R&D Systems) and IFN-γ-AF700 (clone B27) (BD Biosciences) for 30 minutes at 4°C in Perm/Wash buffer (BD Biosciences).

Intracellular transcription factor staining. To assess the expression of intracellular transcription factors, cells were stained for extracellular markers before fixation and permeabilization (Fixation/Permeabilization Buffer Set, eBioscience). Next, cells were stained with anti-human unconjugated Bcl6 (rabbit polyclonal) (Abcam), IRF4-PE-Cy7 (clone 3E4) and IRF8-APC (clone V3GYWCH) (both from eBioscience) for 30 minutes at 4°C in Permeabilization Buffer (eBioscience). To detect the rabbit Bcl6, samples were incubated with

goat anti-rabbit IgG-PE (Invitrogen) for 15 minutes at 4°C in Permeabilization Buffer (eBioscience).

All samples were acquired on a FACS Fortessa instrument (BD Biosciences) and data was analyzed via FlowJo (Treestar).

Lung DC subset FACS sorting

The HLA-DR$^+$ cell fraction was prepurified from total lung cells via the MACS HLA-DR$^+$ purification kit according to manufacturer's protocol (Miltenyi Biotec). HLA-DR$^+$ cells were stained with Aqua LIVE/DEAD, anti-human CD45, HLA-DR, Lineage (CD3ε, CD19, CD56, CD66b), CD11c, CD16, CD141, CD172a, CD1c, CD14 as previously described in this online methods section. Subsequently, DC subsets were sorted with a FACS Aria III instrument (BD Biosciences).

Blood naïve CD4$^+$ T cell isolation and CFSE labeling

Peripheral blood was collected from healthy subjects via venous puncture in Gothenburg, Sweden, under written informed consent. The study was reviewed and approved by the ethical committee/review board in Gothenburg, Sweden, according to the Declaration of Helsinki (number 033-10). Peripheral Blood Mononuclear Cells (PBMC) were prepared by blood centrifugation on a Ficoll gradient (Lymphoprep, Greiner Bio-One). PBMCs were viability frozen in Fetal Calf Serum (FCS) with 10% dimethyl sulfoxide (DMSO) (both Invitrogen) until lung tissue was obtained from the Sahlgrenska Hospital (Gothenburg, Sweden). Naïve CD4$^+$ T cells were isolated from thawed PBMC aliquots by negative selection using the Human Naïve CD4$^+$ T Cell Isolation Kit according to the manufacturer's instructions (Miltenyi Biotec). After isolation, cells were stained with 0,25μM CarboxyFluorescein Succinimidyl Ester (CFSE) (eBioscience) for 10 minutes at room temperature in PBS

(Invitrogen). $CD4^+$ T-cell purity and viability were assessed before each experiment via flow cytometry.

Mixed Leukocyte Reaction (MLR)

Sorted lung DC (5000) were co-cultured with purified CFSE-labeled allogeneic naïve blood $CD4^+$ T-cells (25000) in RPMI medium supplemented with Penicillin/Streptomycin, L-Glutamine and 10% heat-inactivated FCS (all from Invitrogen). After 4 days or 6-7 days, intracellular Bcl6 expression and intracellular IL-21, CXCL13 and IFN-γ levels respectively, were analyzed via flow cytometry as previously described in this online methods section. In some experiments, 1µg/ml anti-human OX40L (oxelumab) or IgG isotype control (both from Biovision) was added.

RNAscope of GOLD IV COPD lung TLO

Lung tissue biopsies were collected, fixed in formalin, dehydrated and embedded in paraffin according to standard protocol. Blocks were cut into 4 µm sections and placed on superfrost plus glasses (ThermoFischer scientific). RNAscope 2.5 LS Duplex *in situ* hybridization was performed according to manufacturer´s protocol (Advanced Cell Diagnostics, Newark, CA) on a Leica Bond Rx autostainer (Leica). Heat induced epitope retrieval was performed for 15 minutes at 95°C using ER2 and protease was applied for 15 minutes. Probes used were: Hs-CD19 and Hs-CH25H. Chromogens applied were bond polymer define detection (brown) and bond polymer refine red detection (both Leica Biosystems) and sections were counterstained with hematoxylin. Slides were mounted using pertex mounting medium and scanned on an aperio scan scope at 20x magnification.

Fluorescence imaging of GOLD IV COPD lung TLO

Lung tissue biopsies were collected and embedded in OCT. Blocks were cut into 4 µm sections and placed on superfrost plus glasses (ThermoFischer scientific). Samples were fixed in aceton (Sigma-Aldrich) for 15 minutes at room temperature. Subsequently, samples were blocked with IHC/ICC Blocking Buffer (eBioscience) for 15 minutes at room temperature. Afterwards, samples were stained with CD3ε-AF647 (clone UCHT1), CD11c-FITC (clone B-ly6) (both BD Biosciences), CD19-Biotin/AF594 (clone HIB19), CD1c-Biotin/AF542 (clone L161) (both Biolegend) and Hoechst nuclear staining (Thermofisher Scientific). Biotin pre-labeling with fluorochromes was performed using the Flexistain™ labeling kit according to the manufacturer's protocol (Kromnigon AB, Sweden). Microscopy images were acquired using an LSM 880 system (Carl Zeiss Microscopy, Germany) equipped with a Zeiss Image Z.1 microscope, Plan-Apochromat 40x/1,3 objective (Carl Zeiss Microscopy, Germany). Brightness and contrast were adjusted using the Zen software (Black ed. v. 2,3, Carl Zeiss Microscopy, Germany).

Statistics

Statistical analyses were calculated with GraphPad Prism (version 8) (GraphPad Software Inc, US) and the tests used are mentioned in the figure legends. *P* values less than 0,05 were considered as significant.

References

1. Pauwels RA, Buist AS, Calverley PM, Jenkins CR, Hurd SS, Committee GS. Global strategy for the diagnosis, management, and prevention of chronic obstructive pulmonary disease. NHLBI/WHO Global Initiative for Chronic Obstructive Lung Disease (GOLD) Workshop summary. *Am J Respir Crit Care Med* 2001; 163: 1256-1276.
2. Kim D, Langmead B, Salzberg SL. HISAT: a fast spliced aligner with low memory requirements. *Nat Methods* 2015; 12: 357-360.
3. Liao Y, Smyth GK, Shi W. featureCounts: an efficient general purpose program for assigning sequence reads to genomic features. *Bioinformatics* 2014; 30: 923-930.
4. Patro R, Mount SM, Kingsford C. Sailfish enables alignment-free isoform quantification from RNA-seq reads using lightweight algorithms. *Nat Biotechnol* 2014; 32: 462-464.
5. Villani AC, Satija R, Reynolds G, Sarkizova S, Shekhar K, Fletcher J, Griesbeck M, Butler A, Zheng S, Lazo S, Jardine L, Dixon D, Stephenson E, Nilsson E, Grundberg I, McDonald D, Filby A, Li W, De Jager PL, Rozenblatt-Rosen O, Lane AA, Haniffa M, Regev A, Hacohen N. Single-cell RNA-seq reveals new types of human blood dendritic cells, monocytes, and progenitors. *Science* 2017; 356.
6. Zilionis R, Engblom C, Pfirschke C, Savova V, Zemmour D, Saatcioglu HD, Krishnan I, Maroni G, Meyerovitz CV, Kerwin CM, Choi S, Richards WG, De Rienzo A, Tenen DG, Bueno R, Levantini E, Pittet MJ, Klein AM. Single-Cell Transcriptomics of Human and Mouse Lung Cancers Reveals Conserved Myeloid Populations across Individuals and Species. *Immunity* 2019; 50: 1317-1334 e1310.
7. Kolde R, Vilo J. GOsummaries: an R Package for Visual Functional Annotation of Experimental Data. *F1000Res* 2015; 4: 574.

Supplemental figure legends

Figure E1: Human non-obstructed lungs contain a highly heterogeneous myeloid cell compartment. (A) Gating strategy for isolating different $Lin^-HLA\text{-}DR^+$ subsets from non-obstructed peritumoral lung resections. Representative flow cytometry plots showing identification of the different DC subsets in human non-obstructed peritumoral lung tissue. Within the viable $CD45^+Lin^-HLA\text{-}DR^+$ cell gate, pDC were identified as $CD11c^-CD123^+$. cDC1 were $CD16^-CD11c^+CD172a^-CD141^+$ while cDC2 were $CD16^-CD11c^+CD172a^+CD1c^+$. Furthermore, $CD14^+$ monocytes were $CD16^-CD11c^+CD172a^+CD1c^-CD14^+$ and $CD16^+$ monocytes were gated as $CD16^+CD11c^+$ cells containing both $CD16^+CD14^-$ and $CD16^+CD14^+$ fractions. Finally, a $Lin^-HLA\text{-}DR^+$ population was found that scored negative for all markers included in the flow cytometry panel. This population was considered as unidentified (un). Shown are representative dot plots from 3 donors (B) *t*-SNE feature plots of the indicated genes defining expression levels in the different clusters. Each dot represents an individual cell (n=3 donors). (C) Flow cytomtery analysis of the different DC subsets from non-obstructed peritumoral lung resections revealed a $CD14^+$ cDC2 fraction and heterogeneous FcεRI and CD1a expression within cDC2. Shown are representative histograms from 3 donors. (D) Flow cytometry plots depicting expression of FcεRI, CD1a, IRF8 and IRF4 by $CD1c^+CD14^-$ and $CD1c^+CD14^+$ cDC2. Shown are representative plots of 3 non-obstructed peritumoral lung resections.

Figure E2: Lung cDC2 are the most potent inducers of Tfh-like cell polarization. DC subsets were purified from non-obstructed peritumoral lung resections and co-cultured with allogeneic naïve blood $CD4^+$ T-cells that were prelabeled with CFSE. (A) Percentages of $ICOS^+PD\text{-}1^+$ T-cells (n=10) in the different DC/T-cell co-cultures were determined at d7 of the

co-culture via flow cytometry. Shown are representative flow cytometry plots for the different DC/T-cell co-cultures corresponding to the cumulative data depicted in Figure 2A. (B) Intracellular IL-21 (n=10) and CXCL13 (n=6) staining of $ICOS^+PD\text{-}1^+$ (purple), $ICOS^-PD\text{-}1^+$ (orange), $ICOS^+PD\text{-}1^-$ (blue) and $ICOS^-PD\text{-}1^-$ (black) T-cell subsets in cDC2/T-cell co-cultures after restimulation with PMA and ionomycin in the presence of Golgi-plug and Golgi-stop. Shown are representative flow cytometry plots corresponding to the cumulative data depicted in Figure 2C (C) Proportions of $ICOS^+CXCR5^+$ T-cells in the different DC/T-cell co-cultures were determined at day 4. Shown are representative flow cytometry plots corresponding to the cumulative data depicted in Figure 2E (n=6). (D) Percentages of $PD\text{-}1^{hi}BCL6^{hi}$ cells in $ICOS^+CXCR5^+$, $ICOS^+CXCR5^-$ and $ICOS^-CXCR5^-$ T-cell subsets in the cDC2/T-cell co-cultures were determined via flow cytometry. Shown are representative flow cytometry plots corresponding to the cumulative data depicted in Figure 2F (n=6).

Figure E3: Lung cDC2 are the most potent inducers of Tfh-like cell polarization. DC subsets were purified from non-obstructed peritumoral lung resections and co-cultured with allogeneic naïve blood $CD4^+$ T-cells that were prelabeled with CFSE. (A) Proliferation of T-cells was assessed via flow cytometry at day 7. Shown are representative histograms of $CFSE^{lo}$ T-cell proportions present in the indicated co-cultures and combined data graph in which each symbol represents an individual donor (n=10). (B) Intracellular IFN-γ (n=10) staining of $ICOS^+PD\text{-}1^+$ (purple), $ICOS^-PD\text{-}1^+$ (orange), $ICOS^+PD\text{-}1^-$ (blue) and $ICOS^-PD\text{-}1^-$ (black) T-cell subsets in cDC2/T-cell co-cultures at day 7 after restimulation with PMA and ionomycin in the presence of Golgi-plug and Golgi-stop. Shown are representative flow cytometry plots and combined data graph in which each symbol represents an individual donor. (C) Percentages of $ICOS^+PD\text{-}1^+IFN\text{-}\gamma^+$ T-cells in cDC2/T-cell and cDC1/T-cell co-cultures were determined

after 7 days. Each symbol represents an individual donor (n=10). **p<0.01, ***p<0.001, Tukey's multiple comparison test (A and B) and Student *t*-test (C).

Figure E4: cDC2 from COPD GOLD II lungs display increased potential to promote Tfh-like cell skewing. (A), (B) and (C) cDC2 were isolated from COPD GOLD II peritumoral lung tissues (n=7) and co-cultured with allogeneic naïve $CD4^+$ T-cells that were prelabeled with CFSE. Proportions of $ICOS^+PD\text{-}1^+$ T-cells (A) and $ICOS^+PD\text{-}1^+IL\text{-}21^+$ T-cells (B) were determined at day 7 and compared to cells from non-obstructed peritumoral lung tissues used in Figure 2 (n=10). Shown are representative flow cytometry plots corresponding to the cumulative data depicted in Figure 3A (E4A) and 3B (E4B) respectively. (C) Proliferation of T-cells (% of $CFSE^{lo}$ T-cells) was assessed via flow cytometry at day 7. Shown is combined data graph in which each symbol represents an individual donor. (D) $CD1c^+CD14^+$ fractions within cDC2 from non-obstructed control and COPDII peritumoral lung tissue used in the co-culture experiments presented in Figure 2 and 3. Show is the summary data graph (n=10 for control and n=7 for COPD). (E) Percentages of $ICOS^+PD\text{-}1^+$ Tfh-like cells in peritumoral lung tissue resections of COPD and non-obstructed control subjects determined via flow cytometry. Shown are representative flow cytometry plots corresponding to the cumulative data depicted in Figure 3C (n=6 for controls and n=5 for COPD subjects).

Figure E5: cDC2 exhibit a unique migratory pattern. (A) Surface levels of CXCR5, CXCR4 and EBI2 were measured on cDC2 and cDC1 from non-obstructed peritumoral lung resections via flow cytometry (n=8 for CXCR5, n=5 for CXCR4 and n=7 for EBI2). Shown are representative flow cytometry histograms for each marker and corresponding isotype. Cumulative data of this experiment depicted in Figure 4A. (B) Surface levels of CXCR5, CXCR4 and EBI2 were measured on cDC2 from non-obstructed and COPD peritumoral lung

resections via flow cytometry (control n=8; and COPD n=4 for CXCR5, control n=5; and COPD n=3 for CXCR4 and control n=7; and COPD n=4 for EBI2). Shown is summary data graph for all the markers (mean MFI corrected for background intensity). (C) Surface EBI2 levels on $ICOS^{+}PD\text{-}1^{+}$ (purple), $ICOS^{-}PD\text{-}1^{+}$ (orange), $ICOS^{+}PD\text{-}1^{-}$ (blue) and $ICOS^{-}PD\text{-}1^{-}$ (black) T-cell subsets in the lung measured via flow cytometry. Shown are representative flow cytometry histograms for EBI2 and isotype of corresponding cumulative data depicted in Figure 4B (n=10).

Supplemental Tables

Table E1: Single Cell cluster markers top 20 by logFC

Cluster	Gene	avg_logFC
1	FCER1A	2,088139734
1	CD1C	1,706769549
1	CCL17	1,449676397
1	HLA-DQB1	1,198897632
1	CD1E	1,159336889
1	HLA-DQA1	1,084527054
1	FCGR2B	1,068335054
1	CD1A	1,042954992
1	CLEC10A	1,027904208
1	CD1B	0,950553648
1	MS4A6A	0,930901312
1	HLA-DRB1	0,903968868
1	HLA-DRA	0,902474636
1	PKIB	0,890630909
1	CD86	0,829732946
1	C15orf48	0,82015284
1	SGK1	0,81219212
1	MNDA	0,812000223
1	GPR183	0,807344769
1	YWHAH	0,798773794
2	FN1	2,095765876
2	FABP4	1,596997079
2	MARCO	1,563296564
2	GPNMB	1,478726772
2	MSR1	1,390751001
2	MCEMP1	1,37408424
2	MRC1	1,368984707
2	CTSD	1,359952157
2	CCL18	1,351578234
2	FBP1	1,333490303
2	OLR1	1,215738999
2	APOC1	1,121526259
2	CTSB	1,106845823
2	LTA4H	1,067928201
2	LGALS3	1,05322345
2	GCHFR	1,044764711
2	VSIG4	0,960665094
2	CTSL	0,955551603
2	INHBA	0,955106343
2	FTL	0,95059228
3	HBG2	2,302686561
3	HBG1	2,027885733

3	AC104389.5	1,865440664
3	GAGE1	1,610717586
3	GTSF1	1,424267207
3	TOP2A	1,335903152
3	NMU	1,299328361
3	PRAME	1,280435628
3	HBE1	1,274461074
3	HIST1H1C	1,253113637
3	UQCRH	1,252614609
3	CKS1B	1,153736826
3	STMN1	1,131076794
3	PAGE5	1,129167523
3	KRT18	1,105038367
3	XAGE1A	1,088383961
3	TPX2	1,033839997
3	EPRS	1,024921962
3	CENPF	1,021810842
3	IFITM1	1,011736626
4	GZMB	3,575265882
4	JCHAIN	2,767735764
4	PLAC8	2,105195767
4	CCDC50	1,883419665
4	TCF4	1,859471292
4	C12orf75	1,831600843
4	IGKC	1,808955309
4	TCL1A	1,801589347
4	TSPAN13	1,716220583
4	CLEC4C	1,693808536
4	BCL11A	1,674993584
4	IRF4	1,637598991
4	UGCG	1,568753728
4	SELL	1,502616827
4	PPP1R14B	1,47257052
4	SOX4	1,456868998
4	HBB	1,438319472
4	ALOX5AP	1,389828099
4	CLIC3	1,361646152
4	SLC15A4	1,340439327
5	VCAN	1,879909516
5	THBS1	1,710398277
5	S100A8	1,707046345
5	S100A9	1,440827397
5	IL1B	1,339112206
5	EREG	1,241721323
5	FCN1	1,091242627
5	CD300E	1,050490024
5	CXCL8	1,011534339
5	APOBEC3A	0,876431337

5	SLC11A1	0,84018397
5	BTBD9	0,809890351
5	CNOT11	0,788145477
5	PCDH9	0,753261137
5	LYZ	0,72719212
5	SLC2A3	0,726358945
5	DOCK7	0,725081441
5	RPSAP48	0,719022886
5	AREG	0,716165035
5	NCALD	0,707815369
6	CCL5	3,094512646
6	CD3D	2,545536387
6	CD2	2,251160687
6	TRAC	2,199659021
6	TRBC2	2,065034272
6	CD3G	1,867353038
6	GZMA	1,743103623
6	CD96	1,737923673
6	SYNE2	1,699053241
6	LCK	1,622384641
6	CD52	1,53198628
6	IFNG	1,53013766
6	CLEC2D	1,491061473
6	CD69	1,481444892
6	TRBC1	1,454386996
6	RORA	1,405689794
6	MKI67	1,374739993
6	TNFAIP3	1,301620037
6	TRAT1	1,299873087
6	GNLY	1,295854049
7	FCGR3A	1,721454744
7	FCN1	1,572985976
7	TNFRSF1B	1,285868263
7	LYST	1,271273287
7	MTSS1	1,250671831
7	CTSS	1,235559792
7	SAT1	1,210844606
7	AIF1	1,180556797
7	APOBEC3A	1,117110701
7	LYN	1,090384191
7	COTL1	1,088225378
7	NAMPT	1,066627046
7	MS4A7	1,057457697
7	WARS	1,046454264
7	HCK	0,994740229
7	MAFB	0,95714909
7	CARD16	0,949365146
7	PECAM1	0,920995962

7	POU2F2	0,899423847
7	PSAP	0,899220709
8	C1orf54	2,502920156
8	S100B	2,215423608
8	CPVL	2,05870984
8	WDFY4	2,030191206
8	CPNE3	1,957136877
8	LGALS2	1,665749813
8	SNX3	1,646792957
8	CST3	1,629844392
8	NAPSB	1,60665153
8	IDO1	1,57189014
8	ID2	1,560949215
8	IRF8	1,50888726
8	CLNK	1,473985276
8	CCND1	1,407907195
8	SLAMF7	1,392130385
8	NAAA	1,374342149
8	CLEC9A	1,340110661
8	DNASE1L3	1,339190346
8	RAB7B	1,288662865
8	WFDC21P	1,286948554
9	SCGB3A2	3,795060405
9	SCGB1A1	3,752372645
9	SFTPB	3,513181643
9	SFTPC	3,410659195
9	SLPI	3,237610149
9	BPIFB1	3,006507765
9	SCGB3A1	2,988363079
9	CYB5A	2,353858175
9	PIGR	2,252972921
9	GPRC5A	2,087974649
9	SFTPA1	2,021757317
9	FMO2	1,990456688
9	SFTPA2	1,988487793
9	KRT19	1,877400103
9	FOLR1	1,797672424
9	CXCL17	1,749139084
9	TMC5	1,741303172
9	DNAH5	1,732458055
9	ELF3	1,708781385
9	STEAP4	1,691137143
10	VWF	2,563873467
10	MGP	2,98839516
10	SPARCL1	2,944658372
10	EPAS1	2,867006965
10	IL33	2,614155574
10	TM4SF1	2,581506323

10	CCL21	2,437221467
10	ABI3BP	2,381497238
10	MMRN1	2,356122626
10	ADIRF	2,300596205
10	CAV1	2,290802751
10	PTPRB	2,258068327
10	CTNNAL1	2,252002567
10	CALCRL	2,215405606
10	IGFBP7	2,213770782
10	VCAM1	2,174300302
10	GIMAP7	2,169786669
10	TNFSF10	2,098405801
10	EDN1	2,09597821
10	ADAMTS1	2,082354785
11	CCR7	2,974205214
11	BIRC3	2,682384903
11	LAMP3	2,493221552
11	CCL22	2,414283922
11	TBC1D4	1,811253495
11	IDO1	1,689907394
11	TXN	1,636759411
11	WFDC21P	1,598379937
11	KIF2A	1,572294609
11	DAPP1	1,556414637
11	CCL17	1,522183075
11	NUB1	1,422680026
11	IL7R	1,382598269
11	RASSF4	1,334039962
11	CSF2RA	1,324384725
11	MARCKS	1,322230231
11	CD274	1,307035179
11	C15orf48	1,273655846
11	MARCKSL1	1,269756605
11	BCL2A1	1,267413041
12	CXCL10	3,616408913
12	CCL8	2,755419177
12	GBP1	2,360339823
12	CXCL11	2,235367058
12	CXCL9	2,182283139
12	CCL2	1,808776529
12	C15orf48	1,544114364
12	GBP5	1,497176194
12	IFIT3	1,437316392
12	CALHM6	1,406032207
12	ISG15	1,385695314
12	APOBEC3A	1,376004478
12	STAT1	1,316194086
12	IDO1	1,26595354

12	PLEK	1,180306973
12	LAP3	1,173269394
12	GBP4	1,171045851
12	TFEC	1,025846406
12	ANKRD22	1,023264534
12	SLAMF7	1,021390851
13	HPGDS	3,269991728
13	CPA3	3,249401012
13	MS4A2	3,112447667
13	KIT	2,807435493
13	CD69	2,424658268
13	IL1RL1	2,357782247
13	TPSB2	2,277193757
13	TPSAB1	2,263245984
13	HPGD	2,104334302
13	HDC	2,085005909
13	RHEX	1,992779128
13	SLC18A2	1,987502805
13	RAB27B	1,930387753
13	VWA5A	1,920039685
13	SCGB1A1	1,772399364
13	RGS13	1,772384031
13	PTGS2	1,577393427
13	SLPI	1,501243584
13	ACSL4	1,487190145
13	EGR3	1,472376666
14	FOLR2	2,114128205
14	LYVE1	2,073485389
14	SELENOP	2,056837651
14	SLC40A1	1,998779877
14	RNASE1	1,980077253
14	CXCL3	1,714787741
14	MT1E	1,625695735
14	CD14	1,535402852
14	MT1X	1,51899883
14	CXCL2	1,510258367
14	MT1G	1,468134634
14	F13A1	1,36859711
14	MT2A	1,294103951
14	C3AR1	1,277064909
14	C1QA	1,274293948
14	CD163	1,271227942
14	MSR1	1,269660758
14	CXCL8	1,266401537
14	MAF	1,256446169
14	CCL4	1,238808215

315

Figure E1

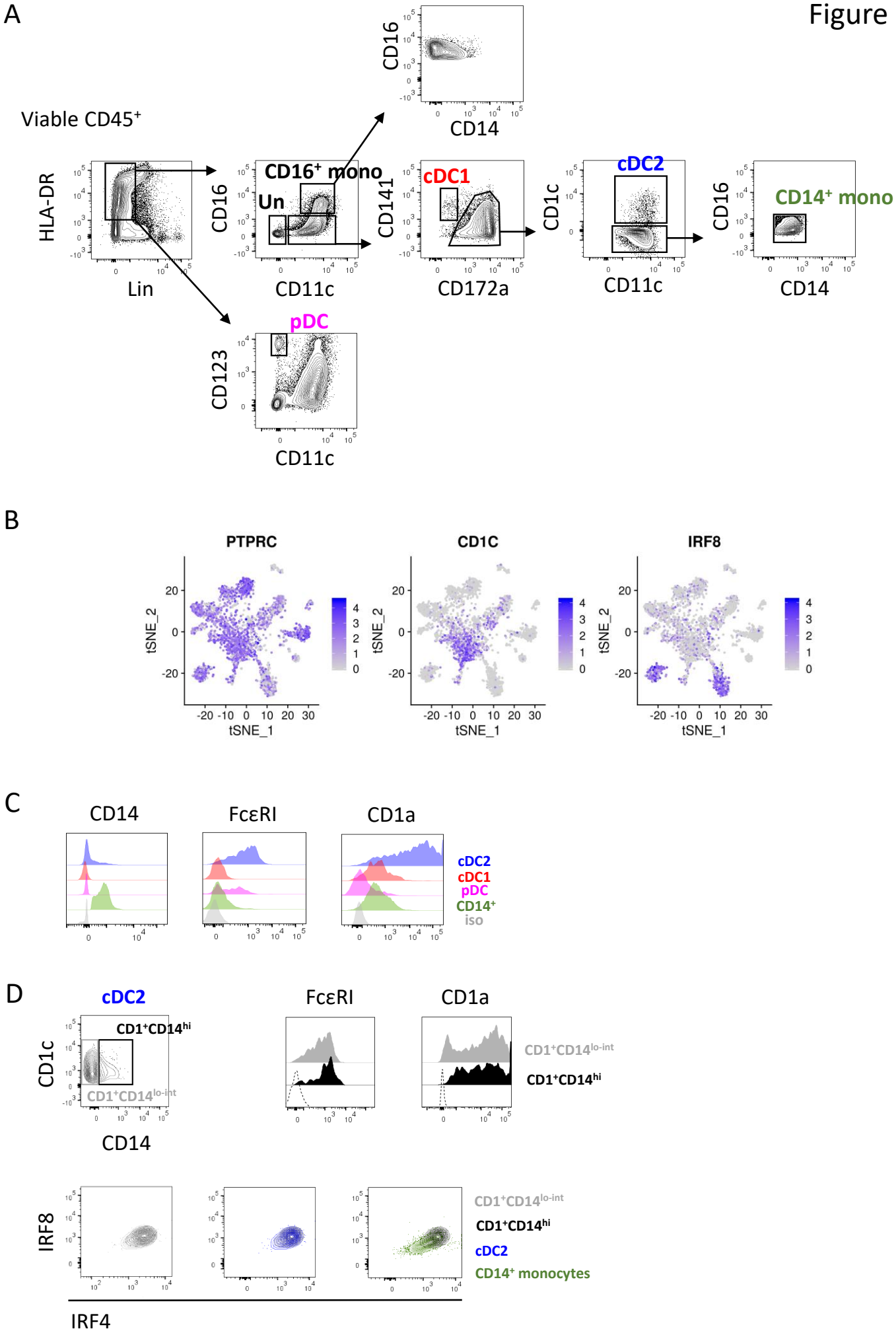
A
Viable CD45+
HLA-DR
Lin
CD16
CD14
CD16+ mono
Un
CD11c
CD141
cDC1
CD172a
CD1c
cDC2
CD11c
CD16
CD14+ mono
CD14
CD123
pDC
CD11c
B
PTPRC
CD1C
IRF8
tSNE_2
tSNE_1
C
CD14
FcεRI
CD1a
cDC2
cDC1
pDC
CD14+
iso
D
cDC2
CD1c
CD1+CD14hi
CD1+CD14lo-int
CD14
FcεRI
CD1a
CD1+CD14lo-int
CD1+CD14hi
IRF8
IRF4
CD1+CD14lo-int
CD1+CD14hi
cDC2
CD14+ monocytes

Figure E2

A

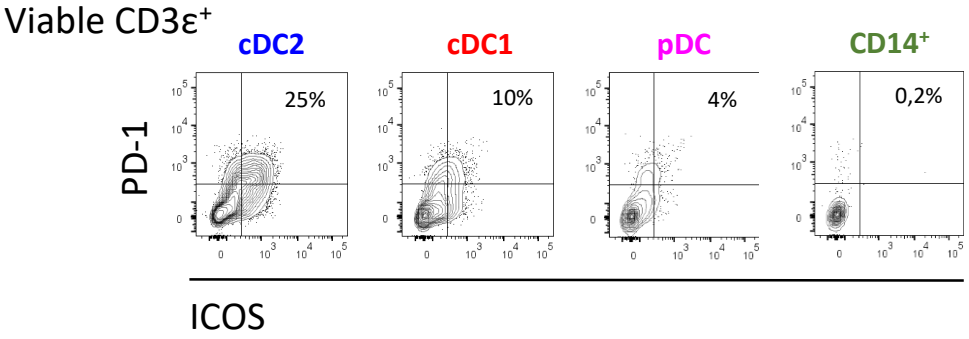

B

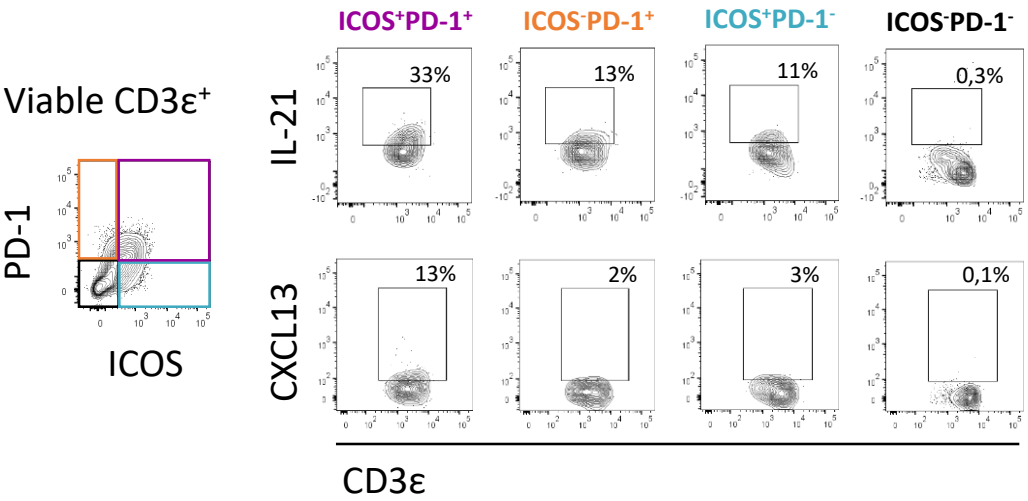

C

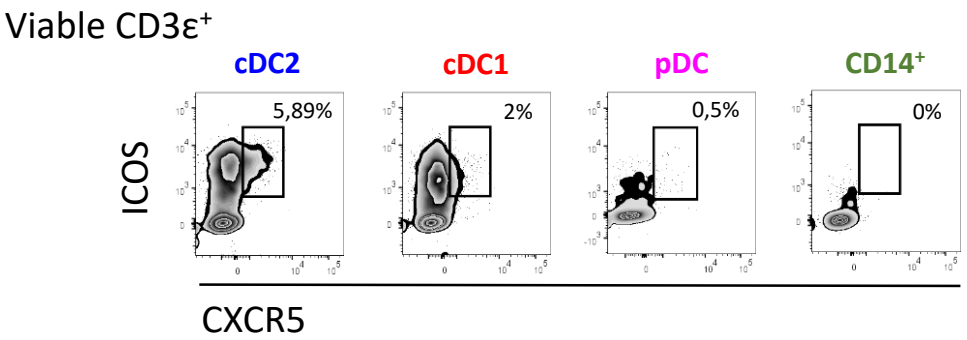

D

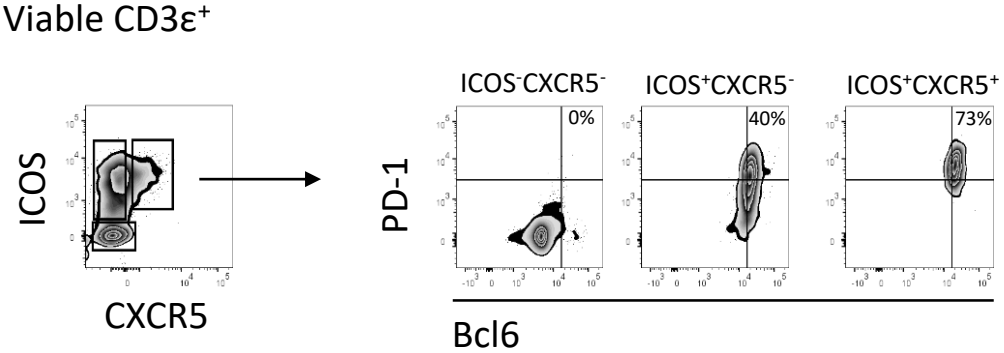

Figure E3

A

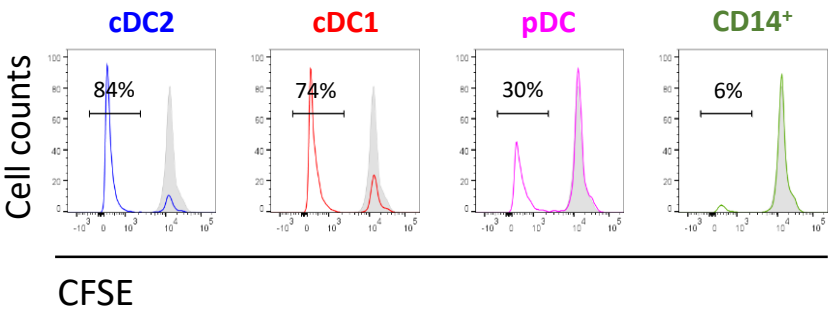

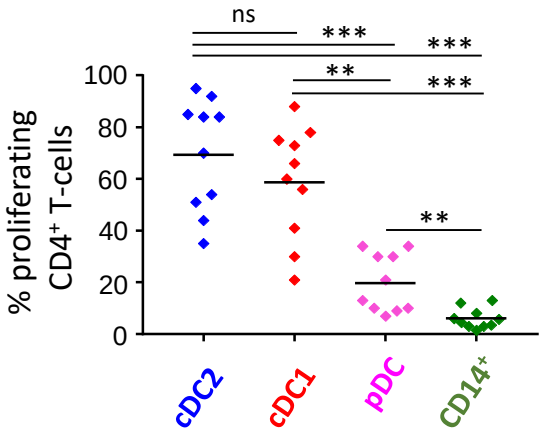

B

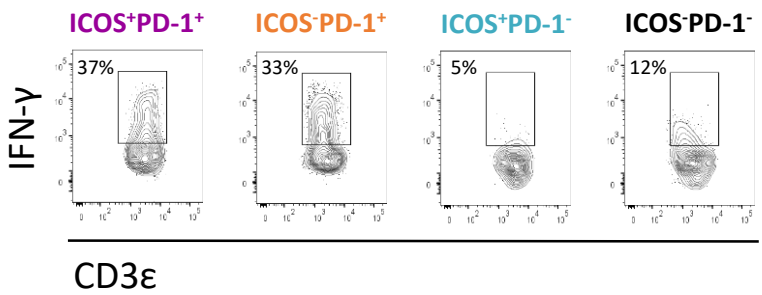

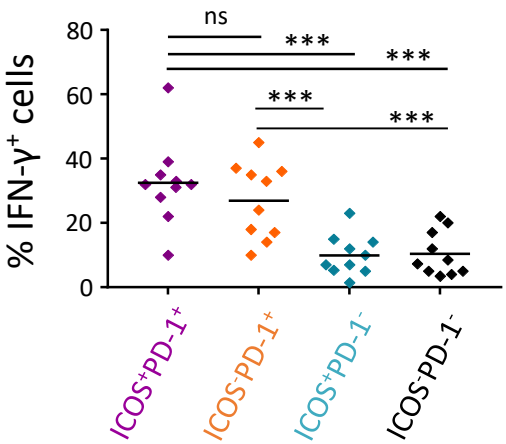

C

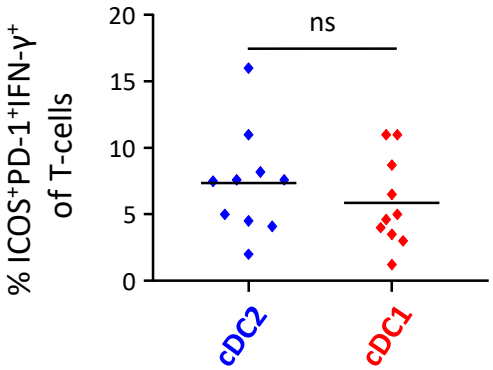

Figure E4

A

Viable CD3ε⁺

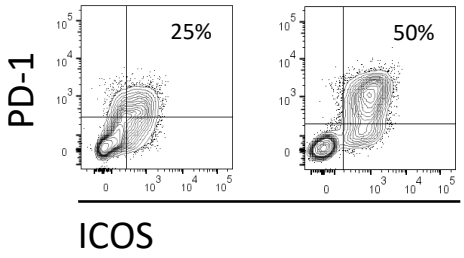

B

Viable CD3ε⁺PD-1⁺ICOS⁺

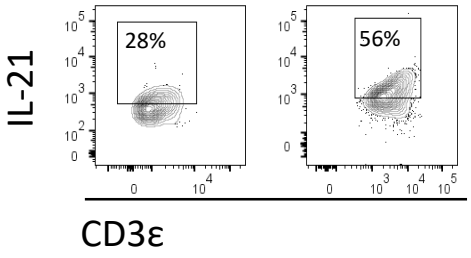

C

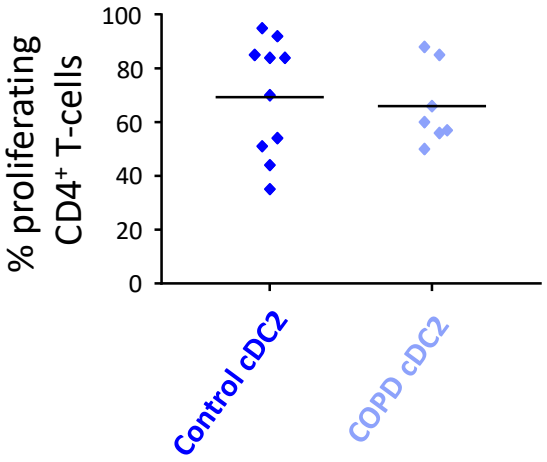

D

CD1c⁺CD14⁺ proportion

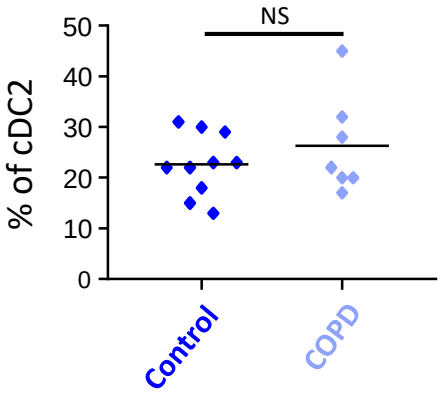

E

Viable CD3ε⁺ CD4⁺

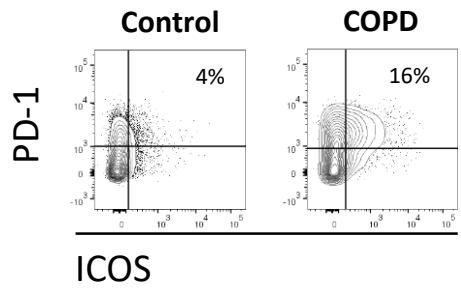

Figure E5

A

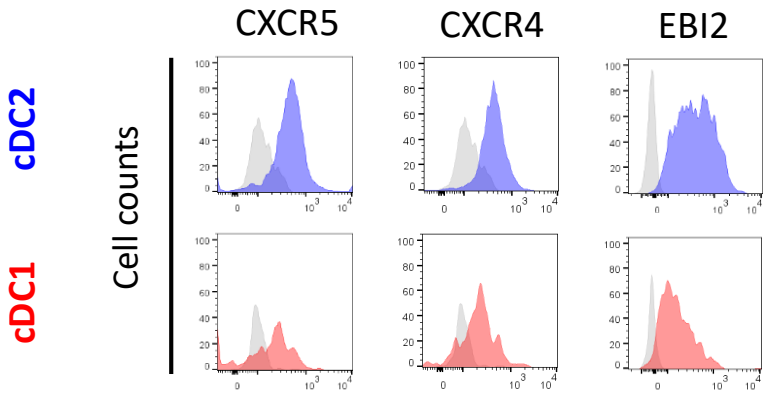

C

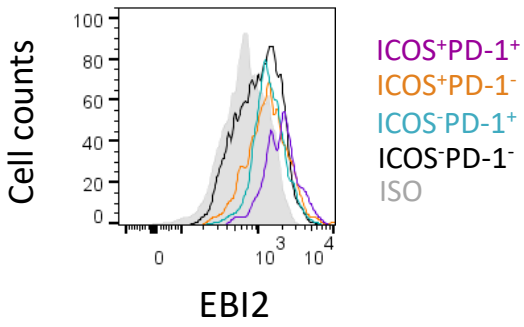

B